Journal of Composite Materials, vol. 44, 2010, 2095-2109

The Tensile Fatigue Behaviour of a Glass-Fiber Reinforced-Plastic Composite Using a Hybrid-Toughened Epoxy Matrix

C.M. MANJUNATHA *

Structural Integrity Group, Structural Technologies Division
National Aerospace Laboratories, Bangalore 560 017, India

S. SPRENGER

Nanoresins AG, Charlottenburger Str. 9
21502 Geesthacht, Germany

A.C. TAYLOR, A.J. KINLOCH

Department of Mechanical Engineering, Imperial College London
South Kensington Campus, London SW7 2AZ, U.K.

ABSTRACT

A thermosetting epoxy-polymer was modified by incorporating 9 wt.% of carboxyl-terminated butadiene-acrylonitrile (CTBN) rubber microparticles and 10 wt.% of silica nanoparticles. The tensile fatigue behaviour at a stress ratio, R = 0.1 for both the neat (i.e. unmodified) epoxy-polymer and the hybrid-epoxy polymer was first investigated. The fatigue life of the hybrid-epoxy

* Corresponding author: Tel. +91-80-2508 6310 ; Fax: +91-80-2508 6301

E-mail address: manjucm@nal.res.in (CM Manjunatha)

polymer was about six to ten times higher than that the neat-epoxy polymer. Secondly, the neat and the hybrid-epoxy resins were infused into a quasi-isotropic lay-up, E-glass fiber fabric via a 'Resin Infusion under Flexible Tooling' (RIFT) set-up to fabricate glass-fiber reinforced-plastic (GFRP) composite panels. The tensile fatigue tests at a stress ratio, R = 0.1 were performed on both of these GFRP composites during which the matrix cracking and stiffness degradation were routinely monitored. The fatigue life of the GFRP composite increased by about six to ten times due to employing the hybrid-epoxy matrix, compared to the neat-epoxy matrix. Suppressed matrix cracking and a reduced crack propagation rate were observed in the hybrid-epoxy matrix, which resulted from the various toughening micromechanisms induced by the presence of both the rubber microparticles and silica nanoparticles. These factors were considered to contribute towards the enhanced fatigue life which was observed for the GFRP composite employing the hybrid-epoxy matrix.

Key words: silica nanoparticle**,** rubber particle**,** glass-fiber composite, fatigue, matrix cracking, epoxy polymers.

INTRODUCTION

Fiber-reinforced plastic (FRP) composites, due to their high specific strength and stiffness, are widely used in various structural applications where they are subjected to constant and variable amplitude fatigue loads in service. Hence, fatigue-durability and high fracture toughness of the composite material are

important requirements in such applications. The majority of engineering composite materials in demanding applications consist of continuous fibers of glass or carbon reinforcement in a thermosetting epoxy-polymer. The epoxy, when polymerised, is an amorphous and a highly cross-linked material. This microstructure of the epoxy polymers results in many useful properties, such as high modulus and failure strength, low creep, etc. However, it also leads to an undesirable property, namely that the epoxy polymer is relatively brittle and has a relatively poor resistance to crack initiation and growth, which adversely affects the overall fatigue and fracture performance of FRP composites when they employ such brittle epoxy matrices.

One of the ways to enhance the mechanical properties of FRPs is to improve the properties of the epoxy matrix by incorporating second-phase fillers in the resin. Various types of micro and nano-sized particulate, fibrous and layered fillers [1-12] have been employed to improve the composite properties. The beneficial effect of the presence of rubber microparticles and silica nanoparticles on the fracture toughness of epoxy polymers and FRPs has recently been investigated extensively [1-5, 7, 8].

In a recent study, Manjunatha et al [13] observed that the addition of 9 wt% rubber microparticles in the epoxy matrix enhanced the fatigue life of a glass fiber reinforced plastic (GFRP) composite by about three times. The incorporation of 10 wt% silica nanoparticles in the epoxy matrix of a GFRP composite has also been shown to have a similar effect in that the fatigue life is enhanced by about three times [14]. Although previous work has shown that [5,7] the fracture toughness increases significantly in a FRP composite with a hybrid-epoxy matrix, i.e. a matrix containing both the rubber

microparticles and silica nanoparticles, detailed studies on the fatigue behaviour of FRP composite using such hybrid-epoxy matrices have not been reported. Hence, the main aim of the present investigation was to study the stress-controlled, constant-amplitude, tensile fatigue behaviour of a GFRP composite employing a hybrid-epoxy matrix. An emphasis was placed on identifying the micromechanisms of the fatigue damage processes.

EXPERIMENTAL

Materials and Processing

The materials were based upon a single-component hot-cured epoxy formulation. The epoxy resin was a standard diglycidyl ether of bis-phenol A (DGEBA) with an epoxy equivalent weight (EEW) of 185 g/mol, 'LY556' supplied by Huntsman, Duxford UK. The silica (SiO_2) nanoparticles were obtained as a colloidal silica sol with a concentration of 40 wt.% in a DGEBA epoxy resin (EEW = 295 g/mol) as 'Nanopox F400' from Nanoresins, Geesthacht, Germany. The reactive liquid rubber, which gives rises to the micrometer-sized spherical rubber particles upon curing of the formulation, was a carboxyl-terminated butadiene-acrylonitrile (CTBN) rubber. It was supplied by Emerald,, Cleveland, USA, and was 'Hycar CTBN 1300 x 8' with a number-average molecular weight of 3550 g/mol and an acrylonitrile content of 18 wt.%. This was pre-reacted with the DGEBA resin to give a 40 wt.% CTBN-epoxy adduct: 'Albipox 1000' (EEW =330 g/mol) from Nanoresins, Geesthacht, Germany. The curing agent was an accelerated methylhexahydrophthalic acid anhydride, 'Albidur HE 600' (AEW =170 g/mol), also supplied by Nanoresins. The E-glass fibre cloth was a non-crimp-fabric

(NCF) roll with two layers of fibers arranged in the $\pm 45^0$ pattern with an aerial weight of 450 g/m^2 from SP Systems, Newport, UK.

The required quantity of the neat DGEBA epoxy resin was weighed and degassed at -1 atm. and 50 ^{0}C. The calculated quantities of silica nanoparticle epoxy-resin and CTBN-epoxy adduct, to give the required level of 10 wt.% added silica and 9 wt.% of CTBN rubber, respectively in the final resin, were also individually weighed and degassed. All the resins were then mixed together and the value of the EEW of the blend was measured via titration. The stiochiometric amount of curing agent was added to the mixture, stirred and degassed once again. The resin mixture was then used to prepare both the bulk epoxy-polymer sheets and the GFRP composite panels. Typically, to prepare a 500 ml (580 g) of the hybrid-resin mixture, about 104 ml (146 g) of Nanopox, 122 ml (131 g) of Albipox, 67 ml (78 g) of LY556 and 207 ml (224 g) of HE600 were used.

To manufacture the epoxy-polymer sheets, the resin mixture was poured into release-coated steel moulds. The filled mould was then placed in a circulating air oven and the temperature was ramped to 100 ^{0}C at 1 ^{0}C/min, cured for 2 hours, again ramped to 150 ^{0}C at 1 ^{0}C/min and post-cured for 10 hours.

The GFRP composite panels were manufactured by the 'Resin Infusion under Flexible Tooling' (RIFT) technique [15]. E-glass fibre non-crimp fabric cloth pieces, about 330 mm square, were cut and laid up in a quasi-isotropic sequence $[(+45/-45/0/90)_s]_2$ with a fluid distribution mesh. The resin mixture was infused into the glass-cloth lay-up at 50^{0}C and -1 atm. Once the infusion was complete, the laminate was cured using the same curing schedule as for

the epoxy polymers, maintaining the vacuum throughout the curing cycle. The resulting GFRP composite laminates, with the neat (i.e. unmodified) and modified matrices were about 2.5-2.7 mm thick and had a fiber volume fraction of about 57%.

Bulk Epoxy Microstructure

Atomic force microscopy (AFM) using a 'multimode' scanning probe microscope from Veeco, UK, equipped with a 'J' scanner and a 'Nanoscope IV' controller was used to observe the microstructure of the hybrid-epoxy polymer. A smooth surface of the epoxy polymer was first prepared by cutting a sample in an ultra-microtome at room temperature. The scans were performed in tapping-mode using silicon probes, and both height and phase images were recorded. The AFM phase images of the modified epoxy polymer are shown in Figure 1. The rubber microparticles were evenly distributed and had an average size of 0.5 to 1 μm. The silica nanoparticles of about 20 nm in diameter [3] were somewhat agglomerated to give a 'necklace-type' structure with an average width of about 1 μm.

Tensile Properties

The tensile properties of the epoxy polymers and GFRP composites were determined according to ASTM D638 [16] and ASTM D3039 [17] test standard specifications, respectively. A schematic diagram showing the dimensions of the test specimen is shown in Figure 2. All the tensile tests were performed using a 100 kN computer controlled screw-driven test machine with a constant crosshead speed of 1 mm/min. The average tensile

properties, determined from five tests on each material, are shown in Table 1. The ultimate tensile strength (UTS) and modulus were decreased by about 12% and 10.5% respectively for the polymer epoxy due to the addition of the silica and rubber particles. However, for the tensile properties of the GFRP composite, the UTS was observed to increase by about 4% and the modulus decrease by about 9.5% for the GFRP composite employing the hybrid-epoxy matrix, compared to the composites employing the neat-epoxy matrix.

Fatigue Testing

The fatigue test specimens, as shown in Figure 2, were prepared from the epoxy-polymer sheets and GFRP composite panels. The sharp edges of the epoxy-polymer test specimens were slightly rounded off with emery paper, before testing, to avoid any stress concentration effects. The fatigue tests were performed as per ASTM D3479M-96 test standard specifications [18], using a 25 kN computer-controlled servo-hydraulic test machine. The tests were conducted at a stress ratio (R), $\sigma_{min} / \sigma_{max} = 0.1$, with a sinusoidal waveform at a frequency, ν = 1 to 3 Hz. The test frequency was kept below 3 Hz to prevent thermal effects leading to reduced fatigue lives [19-21].

The load versus displacement data for one complete load cycle was obtained at specified regular intervals during the fatigue test for stiffness analysis [22]. About fifty pairs of load/displacement data in the central portion of the rising half of load cycle were used to perform the regression analysis. For comparative purposes, the normalised stiffness of the specimen was

defined as the ratio of initial stiffness (obtained in the first cycle) to the measured stiffness at any given load cycle.

Measurement of Crack Density

Due to the translucent nature of the GFRP composite, the development of fatigue damage (e.g. matrix cracks and delaminations) was visible in the gage section of the specimen, under an illuminated-light background. Detailed investigations of matrix cracking was performed during one of the fatigue tests (at σ_{max} = 150 MPa) for the GFRP composites based upon both the neat and the hybrid-epoxy matrices.

About 25 mm x 25 mm area at the centre of the gage section of the test specimen was marked and the specimen was mounted in the servo-hydraulic test machine and fatigue cycles applied. After the application of a specified number of load cycles, the test was stopped, the specimen dismounted and the matrix cracks in the marked area were photographed under a transmitted-light background. The specimen was then re-mounted and the test continued. This procedure was continued until the specimen failed.

A typical sequence of photographic images obtained for the GFRP composite with the neat-epoxy matrix is shown in Figure 3. The virgin sample with no matrix crack is on the far left. The polyester binding yarns in both 0^0 and $\pm 45^0$ directions can be easily recognized (i.e. as faint thick lines) but the E-glass fibres are not visible. With increasing load, cracks develop in the $+45^0$, -45^0 and 90^0 directions and become visible as dark lines in the respective directions. The higher the number of fatigue cycles, the greater the

number of cracks formed. Similar observations of such a matrix cracking sequence in a GFRP composite under fatigue has been reported earlier [23].

Although, cracks in the 90^0 ply were observed in some images, they could not be consistently observed in all the photographs, due to the greater depth of this ply from the surface and also due to the reduced transparency resulting from the addition of particles. However, Gagel et al [23] observed that the stiffness of the composite in the first two stages of its fatigue life correlated strongly with the density of the cracks in the $\pm 45^0$ plies, and only relatively weakly with the presence of the 90^0 ply cracks. Hence, only the cracks in the $\pm 45^0$ plies were considered for analysis in the present investigation.

For the purpose of analysis, the crack density (CD), defined as the number of cracks per unit length, was determined by counting the visible cracks in the $\pm 45^0$ plies on an arbitrarily chosen line drawn on such images. Six such measurements were made on each of the photographic images and the average value of the CD was obtained. It may be noted that there is some uncertainty on the accuracy of such measurements, since the depth of focus may influence the absolute value of the CD measurements. Hence, the CD measurements reported here are used only for comparative, qualitative purposes.

RESULTS AND DISCUSSION

Fatigue Behaviour of the Epoxy Polymers

The constant-amplitude, tension-tension, cyclic-fatigue test results obtained for the bulk neat- and hybrid-epoxy polymers at a stress ratio, R=0.1 are shown in Figure 4. It may be clearly seen that, for any given maximum cyclic stress, the fatigue life of the hybrid-epoxy polymer is higher than that of the neat-epoxy polymer. A fatigue life enhancement of about six to ten times in the hybrid-epoxy polymer is observed over the entire range of stress levels investigated. These results agree with previous studies which also have shown that such nano-modified epoxies exhibit a higher fatigue life compared to the respective neat (i.e. unmodified) polymer [10,12].

The experimental data for the stress-life (S-N) curves of the epoxy polymers shown in Figure 4 were fitted to Basquin's law [24]:

$$\sigma_{max} = \sigma_f' (N_f)^b \quad (1)$$

where, σ_f' is the fatigue strength coefficient (FSC) and 'b' is the fatigue strength exponent (FSE). The values of FSC and FSE determined for both the neat-and the hybrid-epoxy polymers are shown in Table 2. The addition of particles increased the FSC and FSE values by about 18.5% and 6.7% respectively.

The fatigue fracture surface of the epoxy polymers was sputter coated with a thin layer of platinum and observed using a high-resolution scanning-electron microscope fitted with a field-emission gun (FEG-SEM). The FEG-SEM images of both the neat and hybrid-epoxy polymers are shown in Figure 5. The neat epoxy shows (Figure 5 (a)) a relatively smooth fracture surface and is devoid of any indications of large-scale plastic deformation. However, the hybrid-epoxy polymer (Figure 5 (b) and (c)) exhibits a relatively rough

fracture surface with distinctly different features. The cavitation of the rubber microparticles and the associated plastic deformation of the surrounding material are evident in Figure 5(b). Also, a cluster of voids formed due to debonding of silica nanoparticles is observed (Figure 5 (c)). The measured average size of these voids was about 30 nm. This observation indicates that the plastic void growth had occurred during fatigue crack propagation after the silica nanoparticles had debonded.

The toughening micromechanisms in rubber-modified epoxy polymers have been extensively investigated [25-31]. Essentially, the cavitation of the rubber particles leads to enhanced plastic-shear deformation of the epoxy polymer via shear banding and void growth in the epoxy. This energy-dissipating micromechanism has been shown to reduce the crack propagation rates significantly in a rubber-modified epoxy-polymer by up to an order of magnitude [28], hence resulting in an enhanced fatigue life compared with the neat epoxy-polymer.

It has also been observed that the fracture toughness is significantly increased [3] and the fatigue crack growth rate is considerably decreased [32,33] in a silica-nanoparticle modified epoxy. Various toughening micromechanisms have been proposed to explain such observations. Rosso et al [34] observed that the nano-particles caused a high deflection of the crack growth. Zhang et al [35] observed that the nanoparticle induced dimples which might cause energy dissipation. Ma et al [4], proposed the initiation and development of a thin dilatation zone and nano-voids as the dominant toughening mechanisms. However, Johnsen et al [3] identified the major toughening micromechanism as arising from the nanoparticles

debonding and so enabling subsequent plastic void growth of the epoxy polymer.

From the results obtained in the present investigation, it is clear that the micromechanisms of (i) cavitation of the rubber microparticles followed by plastic-deformation and void growth of the epoxy and (ii) silica nanoparticle debonding followed by plastic-deformation and void growth of the epoxy are operative. These toughening micromechanisms will significantly contribute to the enhanced fatigue life of the hybrid-epoxy polymer, compared to the neat-epoxy-polymer.

Fatigue Behaviour of GFRP Composite

The stress-controlled, constant-amplitude, tension-tension fatigue test results at a stress ratio, R = 0.1, obtained for the GFRP composites with neat- and hybrid-epoxy matrices are shown in Figure 6. It may be seen that, over the entire range of stress levels investigated, the addition of particles in the epoxy matrix enhances the fatigue life of the GFRP composites by about six to ten times, compared to using the neat-epoxy matrix. The fatigue properties (FSC and FSE) determined for the composites by fitting the S-N curve data (Figure 6) to eqn. (1) are shown in Table 2. Once again, as observed in the epoxy polymer, the FSC and FSE of the GFRP composites increase; and for the GFRP composites by about 15.6% and 3.7% respectively due to the hybrid-epoxy matrix being employed as opposed to the neat matrix. However, the increase is less marked for the GFRP composites than for the epoxy polymers.

The normalized stiffness variation with load cycles, evaluated for the fatigue test at σ_{max} = 150 MPa for the GFRP composites based upon the neat- and hybrid-epoxy matrices is shown in Figure 7. In general, both GFRP composites exhibit a typical stiffness reduction trend as observed previously in FRP composites [22, 36-40]. The recorded three regions of the stiffness reduction curve are clearly identifiable. It may be noted that the stiffness reductions in 'region I' and 'region II' were quite steep and significant in the neat-matrix GFRP composite, when compared to the GFRP employing the hybrid-epoxy matrix.

Typical transmitted-light photographic images showing cracks in the $\pm 45^0$ plies in both the GFRP composites, obtained after the application of 10,000 load cycles, is shown in Figure 8. The CD in the $\pm 45^0$ plies was determined as a function of the number of fatigue cycles and is shown in Figure 9. In both composites, the CD increased with load cycles and appears to saturate [41]. The saturation level of CD was higher and about 4.5/mm for the neat-matrix GFRP, whereas it was about 1.8/mm for the GFRP with the hybrid-epoxy matrix. This saturation level of the progressive formation of matrix cracks, also termed the characteristic damage state (CDS) [36,38,41], is reached much faster in the neat-matrix GFRP. It is clear from Figure 9 that, for any given load cycle, the GFRP based on the neat matrix possesses a considerably greater CD value than the GFRP employing the hybrid-matrix, over the entire fatigue life of the composite.

The initiation and growth of interlaminar delaminations, particularly from the free edges of the test specimens were observed (Figure 10) with continued fatigue cycling. Such free edge delaminations have been

previously observed in studies of composite fatigue failures [42]. The initiation of delamination damage was visually observed at about 6,000 and 30,000 cycles in the neat- and hybrid-matrix GFRP composites, respectively. The growth of such delamination under fatigue cycling leads to the final failure of the GFRP composites.

Based on the results obtained, the sequence of fatigue damage development leading to final failure and hence defining the fatigue life in the quasi-isotropic lay-up GFRP composites may be briefly described as follows [36,38,43,44]. Initially, in both GFRP composites, matrix cracks develop (Figure 8) in the $\pm 45^0$ off-axis plies due to the cyclic-fatigue loading. The density of these matrix cracks increase (see Figure 9) and the cracks propagate with further continued application of load cycles, resulting in a continuous decrease in the global stiffness of the composite (i.e. in region I of Figure 7). However, when the relatively tough hybrid-epoxy matrix is employed, the extent of matrix cracking is suppressed and the crack density is relatively low in the GFRP with the hybrid matrix (see Figure 9). Now, from the epoxy-polymer fatigue studies, it is clear that fatigue life is enhanced due to reduced crack growth rates in the hybrid-epoxy polymer (see Figure 4 and Figure 5). This reduced cracking in the hybrid-epoxy matrix results in lower degradation of the GFRP with the hybrid matrix under the fatigue loads compared to the neat-matrix (see Figure 7).

The matrix-cracking process continues until reaching the CDS, when the formation of secondary cracks in the epoxy matrix, perpendicular to primary cracks, leads to initiation of interlaminar delaminations (see Figure 10). Further growth of this damage lead to a continued stiffness loss, in

'region II' of Figure 7. Once again, due to reduced delamination/crack growth rates [28,32,33], the stiffness reduction is much slower in the hybrid-matrix GFRP (see Figure 7). It has also been shown that matrix crack-coupled [38] fiber-breaking is an additional fatigue-damage micromechanism which occurs during the entire fatigue life. We believe that such fiber breaks are probably delayed in the GFRP employing the hybrid-epoxy matrix, due to the reduced crack growth rates induced by the presence of the particles. The accumulation and growth of all these various types of damage leads to final fatigue failure of the composites. However, the GFRP employing the hybrid-epoxy matrix exhibits an improved fatigue life compared to that of the GFRP using the neat-epoxy matrix due to the toughening micromechanisms induced by the presence of the rubber microparticles and silica nanoparticles in the former matrix, as described above.

It is noteworthy that although hybrid toughening of epoxy polymer results in significant enhancement of fracture toughness [5,7] and fatigue life [13,14] of composites, the presence of liquid rubber increases the viscosity of the resin which may cause difficulties in producing large sized components. Also, presence of particles reduces the glass transition temperature, T_g slightly and enhance the moisture uptake in hot-wet conditions which may result in reducing the mechanical properties of the material.

CONCLUSIONS

The following conclusions may be drawn based on the results obtained in the present investigation:

1. The cyclic fatigue life of an epoxy polymer modified with 9 wt% CTBN rubber microparticles and 10 wt% silica nanoparticles is about six to ten times higher than that of the neat-epoxy polymer. This arises since the toughening micromechanisms of (i) cavitation of the rubber microparticles followed by plastic-deformation and void growth of the epoxy and (ii) silica nanoparticle debonding followed by plastic-deformation and void growth of the epoxy are operative in the hybrid-epoxy polymer. These toughening micromechanisms will significantly contribute to the enhanced fatigue life of the hybrid-epoxy polymer, compared to the neat-epoxy polymer.

2. The cyclic-fatigue life of the GFRP composite with the hybrid-epoxy matrix, containing 9 wt% CTBN rubber microparticles and 10 wt.% silica nanoparticles, is about six to ten times higher than that of the GFRP composite based on the neat-epoxy matrix. The suppressed matrix cracking and reduced crack-growth rate, arising from the presence of the rubber microparticles and silica nanoparticles in the hybrid-epoxy matrix, lead to the observed enhancement of the fatigue life in the GFRP employing the hybrid-epoxy matrix.

ACKNOWLEDGEMENTS

This work was carried out in the Department of Mechanical Engineering, Imperial College, London, UK. Dr. CM Manjunatha wishes to thank and acknowledge the United Kingdom-India Education and Research Initiative (UKIERI) for the award of a Research Fellowship. He also wishes to thank

Dr. AR Upadhya, Director and Mr. DV Venkatasubramanyam, Head, Structural Technologies Division, National Aerospace Laboratories, Bangalore, India for permitting him to accept the Fellowship and providing their constant support and encouragement during this work. Mr. J Sohn Lee is thanked for his assistance with the FEG-SEM work. The technical support staff members of the Department of Mechanical Engineering and the Composite Centre of Aerospace Department, Imperial College, London are thanked for their assistance with the experimental work.

REFERENCES

[1] Kinloch, A.J., Mohammed, R.D., Taylor, A.C., Eger, C., Sprenger, S. and Egan, D. (2005). The Effect of Silica Nano Particles and Rubber Particles on the Toughness of Multiphase Thermosetting Epoxy Polymers. *J Mater Sci*, **40(18):** 5083-5086.

[2] Fu, S.Y., Feng, X.Q., Lauke, B. and Mai, Y.W. (2008). Effects of Particle Size, Particle/Matrix Interface Adhesion and Particle Loading on Mechanical Properties of Particulate-Polymer Composites. *Composites: Part ,* **39**:933–961.

[3] Johnsen, B.B., Kinloch, A.J., Mohammed, R.D., Taylor, A.C. and Sprenger, S.(2007). Toughening Mechanisms of Nanoparticle-Modified Epoxy Polymers. *Polymer,* **48(2):** 530-541.

[4] Ma, J., Mo, M.S., Du, X.S., Rosso, P., Friedrich, K. and Kuan, H.C. (2008). Effect of Inorganic Nanoparticles on Mechanical Property, Fracture Toughness and Toughening Mechanism of Two Epoxy Systems. *Polymer*, **49:** 3510-3523.

[5] Kinloch, A.J., Mohammed, R.D., Taylor, A.C., Sprenger, S. and Egan, D.J. (2006). The Interlaminar Toughness of Carbon Fiber Reinforced Plastic Composites Using Hybrid Toughened Matrices. *J Mater Sci,* **41(15):**5043-5046.

[6] Chisholm, N., Mahfuz, H., Rangari, V.K., Ashfaq, A. and Jeelani, S. (2005). Fabrication and Mechanical Characterization of Carbon/Sic-Epoxy Nanocomposites. *Comp Struct,* **67:** 115-124.

[7] Kinloch, A.J., Masania, K., Taylor, A.C., Sprenger, S. and Egan, D. (2008). The Fracture of Glass Fiber Reinforced Epoxy Composites Using Nanoparticle Modified Matrices. *J Mater Sci*, **43(3):**1151-1154.

[8] Zheng, Y., Zheng, Y. and Ning, R. (2003). Effects of Nanoparticles SiO_2 on the Performance of Nanocomposites. *Mater Lett,* **57:** 2940-2944.

[9] Gojny, F.H., Wichmann, M.H.G., Fiedler, B., Bauhofer, W. and Schulte, K. (2005). Influence of Nano-Modification on the Mechanical and Electrical Properties of Conventional Fiber-Reinforced Composites. *Compos Part A,* **36:**1525-1535.

[10] Zhou, Y., Pervin, F., Jeelani, S. and Mallick, P.K. (2008). Improvement in Mechanical Properties of Carbon Fabric-Epoxy Composite Using Carbon Nanofibers. *J Mater Proc Tech*, **198:** 445-453.

[11] Haque, A., Shamsuzzoha, M., Hussain, F. and Dean, D. (2003). S2-Glass/Epoxy Polymer Nanocomposites: Manufacturing, Structures, Thermal and Mechanical Properties. *J comp mater,* **37(20):**1821-1837.

[12] Zhou, Y., Rangari, V., Mahfuz, H., Jeelani, S. and Mallik, P.K. (2005). Experimental Study on Thermal and Mechanical Behaviour of Polypropylene, Talc/Polypropylene and Polypropylene/Clay Nanocomposites. *Mater Sci Engg A,* **402:** 109-117.

[13] Manjunatha, C.M., Taylor, A.C., Kinloch, A.J. and Sprenger, S. (2009) The Tensile Fatigue Behaviour of a GFRP Composite With Rubber Particle Modified Epoxy Matrix. *J Rein Plas Compos,* doi:10.1177/0731684409344652

[14] Manjunatha, C.M., Taylor, A.C., Kinloch, A.J. and Sprenger, S. (2009). The Effect of Rubber Micro-Particles and Silica Nano-Particles on the Tensile Fatigue Behaviour of a Glass Fiber Epoxy Composite. *J Mater Sci*, **44:** 342-345.

[15] Summerscales, J. and Searle, T.J. (2005). Low-Pressure (Vacuum Infusion) Techniques for Moulding Large Composite Structures, *Proc IMechE, J Mater: Des Appl***, 219:** 45-58.

[16] Standard Test Method for Tensile Properties of Plastics, ASTM D638-01, Annual book of ASTM Standards, American Society for Testing and Materials, PA, Vol. 8.02, 2003.

[17] Standard Test Method for Tensile Properties of Polymer Matrix Composite Materials, ASTM D3039, Annual book of ASTM Standards, American Society for Testing and Materials, PA, Vol. 15.03, 2003.

[18] Standard Test Method for Tension-Tension Fatigue of Polymer Matrix Composite Materials, ASTM D3479M-96, Annual book of ASTM Standards, American Society for Testing and Materials, PA, Vol. 8.02, 2003.

[19] Mandell, J.F. and Meier, U. (1983). Effect of Stress Ratio, Frequency and Loading Time on the Tensile Fatigue Of Glass-Reinforced Epoxy, In: O'Brien TK, Ed., Long-Term Behaviour of Composites, ASTM STP 813, ASTM International, West Conshohocken, PA, 55-77.

[20] Staff, C.R.(1983). Effect of Load Frequency and Lay-Up on Fatigue Life of Composites. In: O'Brien TK, Ed., Long-Term Behaviour of Composites, ASTM STP 813, ASTM International, West Conshohocken, PA, 78-91.

[21] Sun, C.T. and Chan, W.S. (1979). Frequency Effect on the Fatigue Life of a Laminated Composite, In: Composite Materials: Testing and Design (Fifth Conference), ASTM STP 674, Tsai SW, Ed., ASTM International, West Conshohocken, PA, 418-430.

[22] Lee, J., Fu, K.E. and Yang, J.N. (1996). Prediction of Fatigue Damage and Life for Composite Laminates Under Service Loading Spectra. *Comp Sci Tech*, **56:** 635-648.

[23] Gagel, A., Lange, D. and Schulte, K. (2006). On The Relation Between Crack Densities, Stiffness Degradation and Surface Temperature

Distribution of Tensile Fatigue Loaded Glass-Fiber Non-Crimp-Fabric Reinforced Epoxy. *Comp Part A,* **37**: 222-228.

[24] Buch, A. (1988). Fatigue Strength Calculation. Transtech Publications. Switzerland.

[25] Kinloch, A.J. (2003). Toughening Epoxy Adhesives to Meet Today's Challenges. *MRS Bulletin*, **28(6):** 445-448.

[26] Arias, M.L, Frontini, P.M. and Williams, R.J.J. (2003). Analysis of the Damage Zone Around The Crack Tip For Two Rubber-Modified Epoxy Matrices Exhibiting Different Toughenability. *Polymer,* **44(5):**1537-1546.

[27] Pearson, R.A. and Yee, A.F. (1991). Influence of Particle Size and Particle Size Distribution on Toughening Mechanisms in Rubber Modified Epoxies. *J Mater Sci,* **26(14):** 3828-3844.

[28] Azimi, H.R, Pearson, R.A. and Hertzberg, R.W. (1996). Fatigue of Rubber-Modified Epoxies: Effect of Particle Size and Volume Fraction. *J Mater Sci,* **31(14):** 3777-3789.

[29] Low, I.M. and Mai, Y.W. (1988). Micromechanisms of Crack Extension in Unmodified and Modified Epoxy Resins. *Compos Sci Tech*, **33(3):** 191-212.

[30] Lowe, A., Kwon, A.H. and Mai, Y.W. (1996). Fatigue and Fracture Behavior of Novel Rubber Modified Epoxy Resins. *Polymer,* **37(4):** 565-572.

[31] Imanaka, M., Motohashi, S., Nishi, K., Nakamura, Y. and Kimoto, M. (2009). Crack-Growth Behaviour of Epoxy Adhesives Modified With Liquid Rubber and Cross-Linked Rubber Particles Under Mode I Loading, *Int J Adhesion and Adhesives*, **29(1):** 45-55.

[32] Caccavale, V., Wichmann, M.H.G., Quaresimin, M. And Schulte, K. (2007). Nanoparticle/Rubber Modified Epoxy Matrix Systems: Mechanical Performance in CFRPs. in: AIAS XXXVI Convegno Nazionale, Ischia, Napoli, 4-8 Sept 2007.

[33] Blackman, B.R.K., Kinloch, A.J., Sohn Lee, J., Taylor, A.C., Agarwal, R., Schueneman, G. and Sprenger, S. (2007). The Fatigue and Fracture

Behaviour of Nano-Modified Epoxy Polymers. *J Mater Sci,* **42:** 7049-7051.

[34] Rosso, P., Ye, L., Friedrich, K. and Sprenger, S. (2006). A Toughened Epoxy Resin by Silica Nanoparticle Reinforcement. *J Appl Polym Sci,* **100(3):**1849-1853.

[35] Zhang, H., Zhang, Z., Friedrich, K. and Eger, C. (2006). Property Improvements of in Situ Epoxy Nanocomposites With Reduced Interparticle Distance at High Nanosilica Content. *Acta Mater,* **54(7):**1833-1842.

[36] Talreja, R. (1989). Fatigue of Composite Materials: Damage Mechanisms and Fatigue Life Diagrams. *Proc Roy Soc Lon A,* **378:**559-567.

[37] Hahn, H.T., Kim, R.Y. (1976). Fatigue Behaviour of Composite Laminates. *J Comp Mater,* **10:**156-180.

[38] Case, S.W. and Reifsnider, K.L. Fatigue of Composite Materials. In: Milne I, Ritchie RO, Karihaloo B. Eds., Comprehensive structural integrity. Vol. 4: Cyclic loading and fatigue, 1st edn. Elsevier Science, Amsterdam, 2003.

[39] Tate, J.S. and Kelkar, A.D. (2008). Stiffness Degradation Model for Biaxial Braided Composites Under Fatigue Loading. *Comp Part B* **39(3):**548-555.

[40] Reifsnider, K.L. and Jamison, R. (1982). Fracture of Fatigue-loaded Composite Laminate. *Inter J Fat,* **4(4):**187-197.

[41] Li, C., Ellyin, F. and Wharmby, A. (2003). On Matrix Crack Saturation in Composite Laminates. *Comp Part B,* **34:**473-480.

[42] Case, S.W., Caliskan, A., Iyengar, N. and Reifsnider, K.L. Performance simulation of high-temperature polymeric composite materials using MR Life. In: Proc ASME Aerosp Div-1996 ASME Inter Mech Eng Cong Exp, pp. 375-380.

[43] Reifsnider, K. (1980). Fatigue Behaviour of Composite Materials. *Inter J Frac,* **16(6):**563-583.

[44] Wharmby, A.W., Ellyin, F. and Wolodko, J.D. (2003). Observation on Damage Development in Fiber Reinforced Polymer Laminates Under Cyclic Loading. *Int J Fat,* **25:**437-446.

Figure Captions

Figure 1. The tapping mode atomic force microscopic (AFM) phase images of the hybrid-epoxy polymer.

Figure 2. A schematic diagram showing the dimensions of the tensile and fatigue test specimens.

Figure 3. The transmitted light photographic images of GFRP composite with the neat-epoxy matrix showing the sequence of matrix crack development with fatigue loading.

Figure 4. The stress versus fatigue life (S-N) curves of the neat- and hybrid-epoxy polymers.

Figure 5. The scanning electron micrographs of the fatigue fracture surfaces of the neat- and hybrid-epoxy polymers (crack growth direction is from left to right. σ_{max} = 37 MPa, R = 0.1). (a) neat-epoxy polymer, (b) hybrid-epoxy polymer showing rubber particle cavitation and void growth, and (c) hybrid-epoxy polymer showing voids (circled) due to silica nanoparticle debonding and void growth.

Figure 6. The stress versus fatigue life (S-N) curve of the GFRP composites with a neat- and a hybrid-epoxy matrix.

Figure 7. The normalised stiffness variation with fatigue cycling in GFRP composites with a neat- and a hybrid-epoxy matrix. σ_{max} = 150 MPa, R = 0.1

Figure 8. The transmitted-light photographic images showing the matrix cracking pattern in GFRP composites under fatigue loading. σ_{max} = 150 MPa, N = 10,000 cycles

Figure 9. The variation of the $\pm 45^0$ crack density with fatigue cycles in GFRP composites with a neat- and a hybrid-epoxy matrix.

Figure 10. The interlaminar delaminations observed at the free edges of the test specimen during fatigue testing of the GFRP composite based on the neat-epoxy matrix. σ_{max} = 150 MPa and R = 0.1

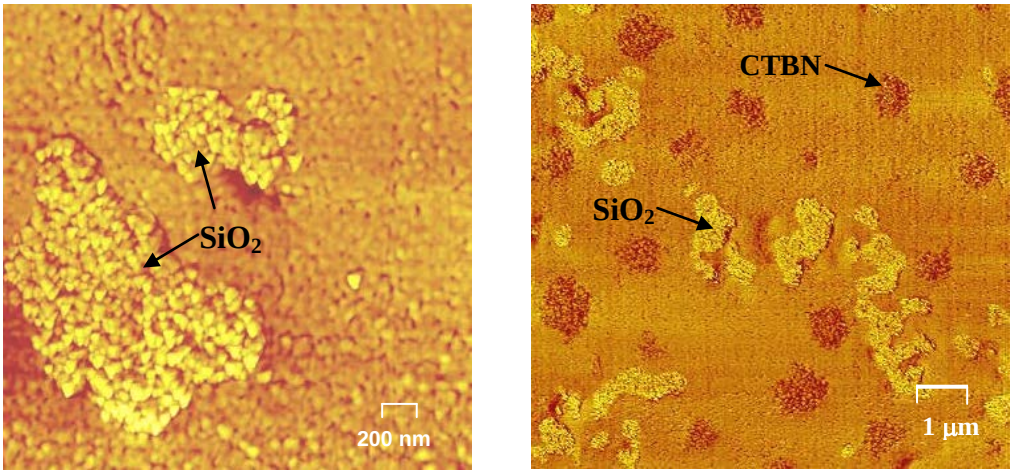

Figure 1

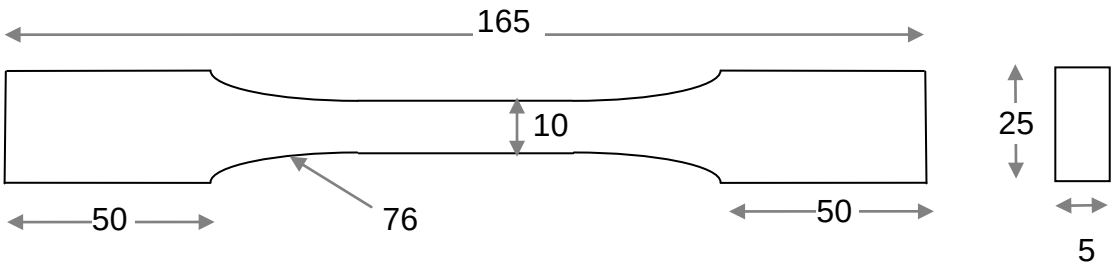

(a) Epoxy polymer

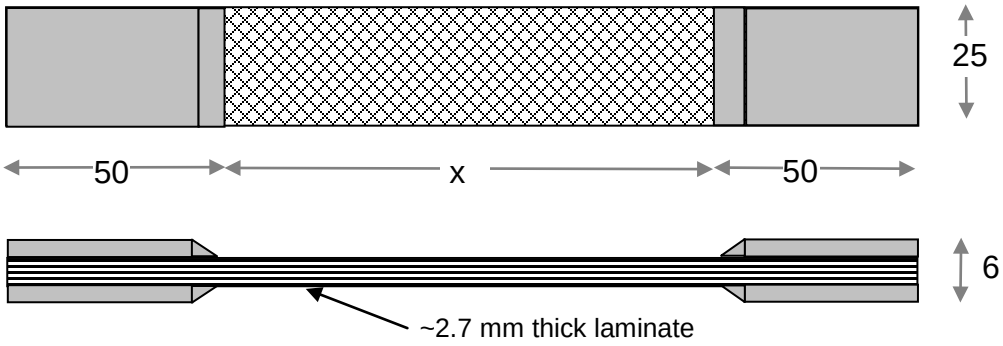

Note: All dimensions are in mm
X= 150mm for tensile tests
X= 50 mm for fatigue tests

(b) GFRP composite

Figure 2

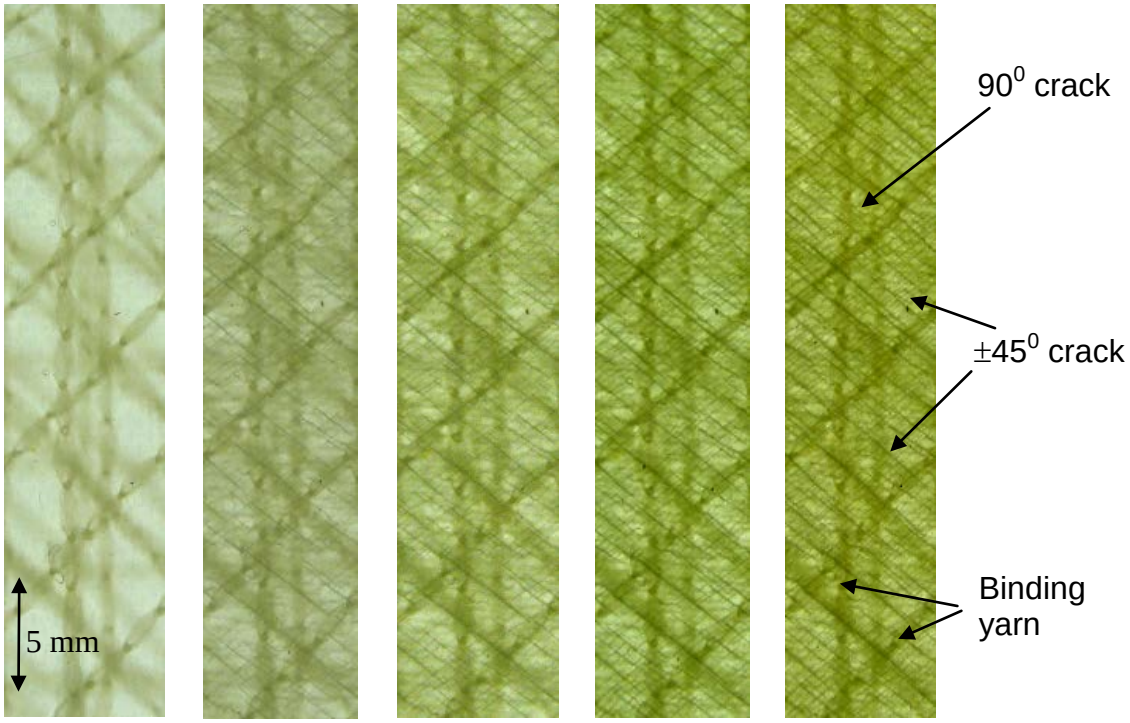

Figure 3

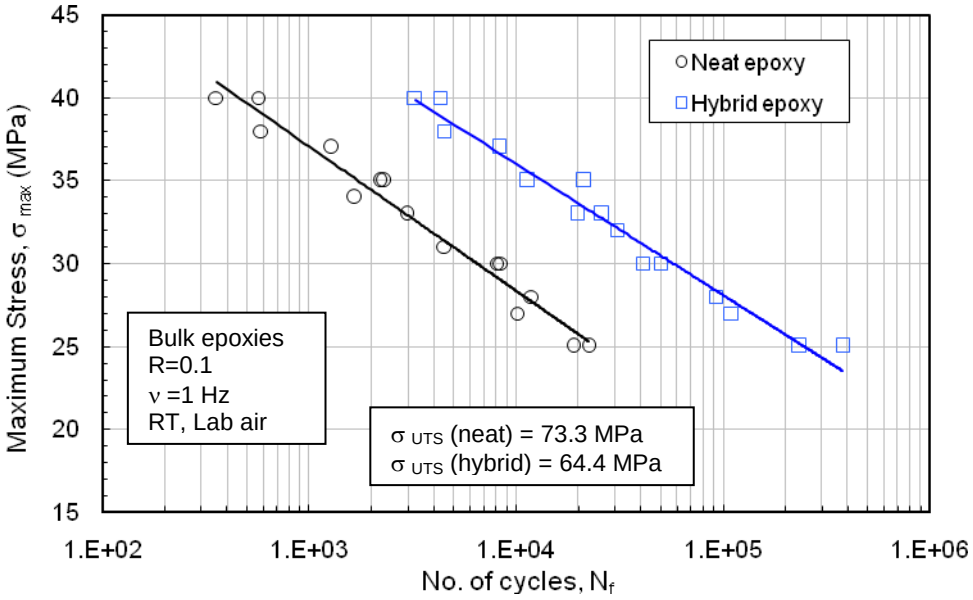
Maximum Stress, σ max (MPa)
45
40
35
30
25
20
15
1.E+02
1.E+03
1.E+04
1.E+05
1.E+06
No. of cycles, Nf
Neat epoxy
Hybrid epoxy
Bulk epoxies
R=0.1
ν =1 Hz
RT, Lab air
σ UTS (neat) = 73.3 MPa
σ UTS (hybrid) = 64.4 MPa

Figure 4.

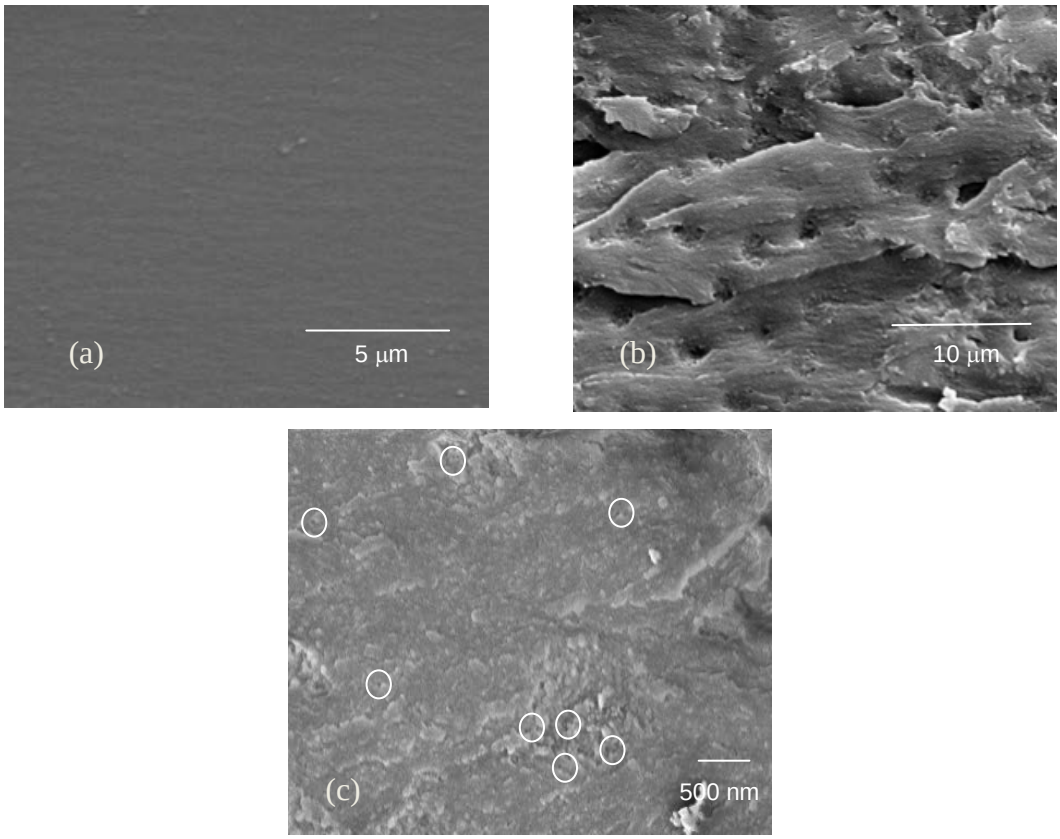

Figure 5

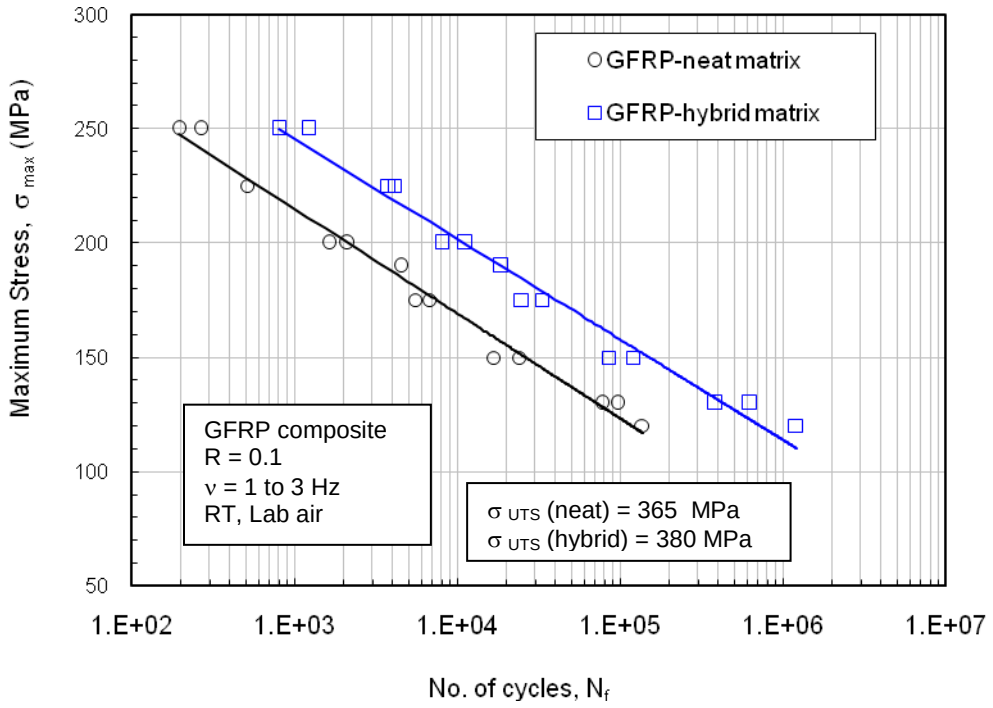
300
250
200
150
100
50
Maximum Stress, σ max (MPa)
1.E+02
1.E+03
1.E+04
1.E+05
1.E+06
1.E+07
No. of cycles, Nf
GFRP-neat matrix
GFRP-hybrid matrix
GFRP composite
R = 0.1
ν = 1 to 3 Hz
RT, Lab air
σ UTS (neat) = 365 MPa
σ UTS (hybrid) = 380 MPa

Figure 6.

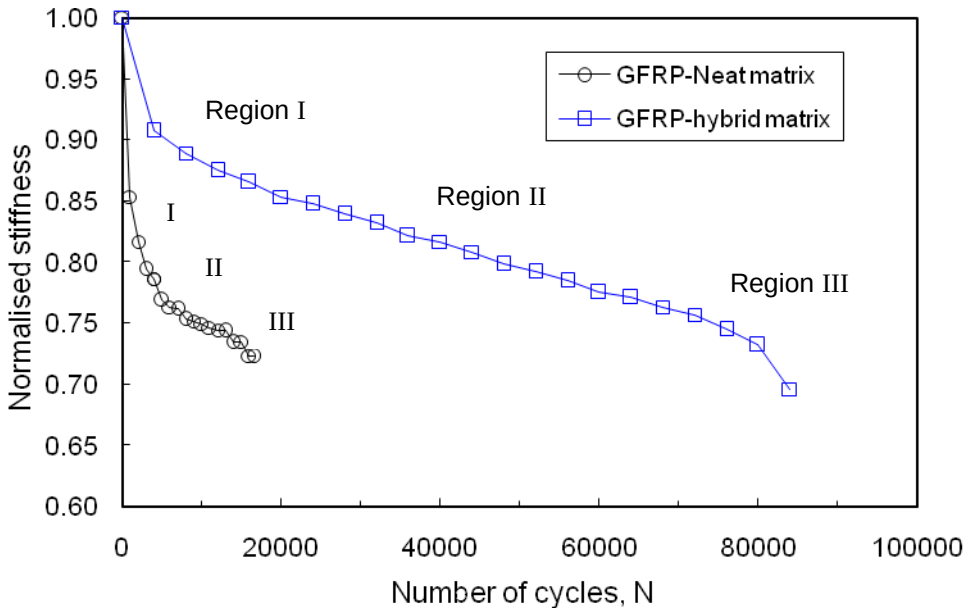
1.00
0.95
0.90
0.85
0.80
0.75
0.70
0.65
0.60
Normalised stiffness
0
20000
40000
60000
80000
100000
Number of cycles, N
GFRP-Neat matrix
GFRP-hybrid matrix
Region I
Region II
Region III
I
II
III

Figure 7.

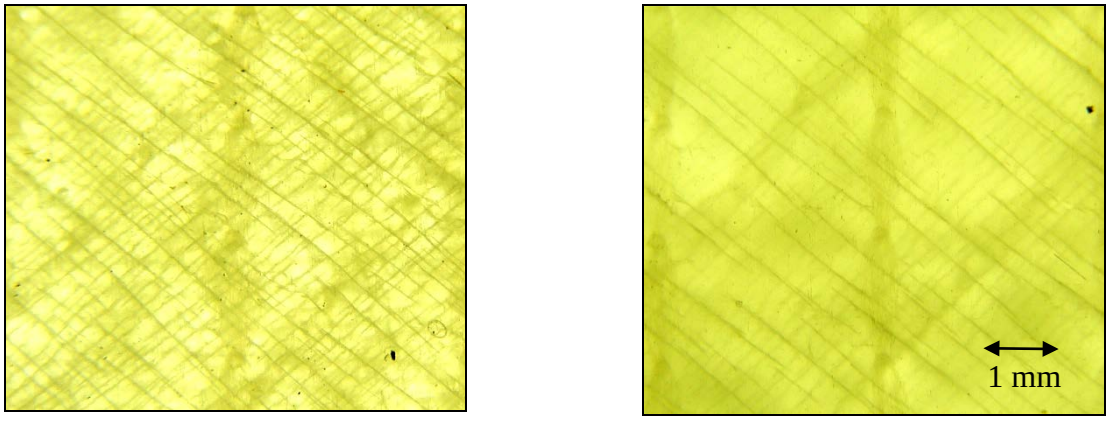

(a) GFRP with the neat-epoxy matrix

(b) GFRP with the hybrid-epoxy matrix

Figure 8

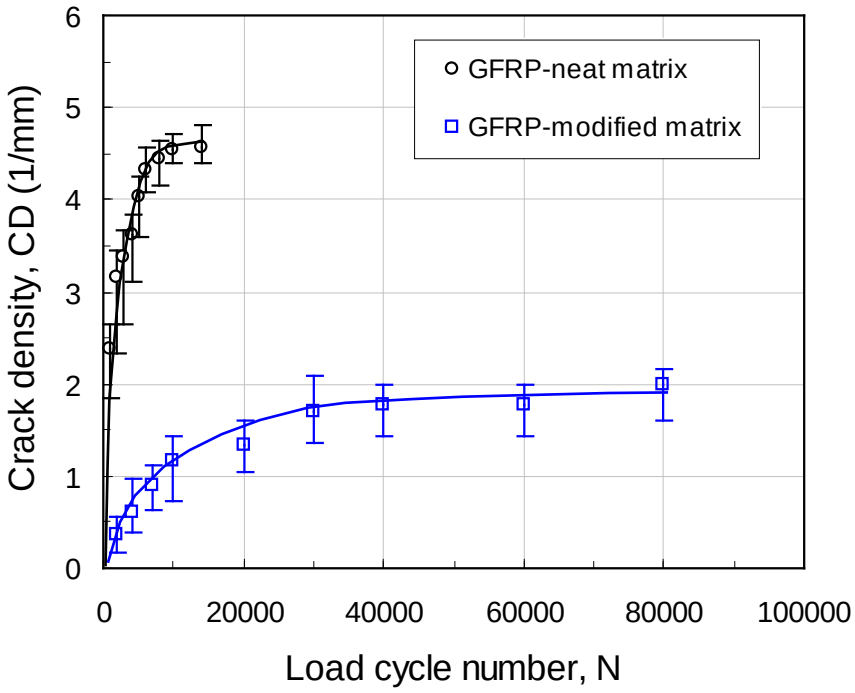
GFRP-neat matrix
GFRP-modified matrix
Crack density, CD (1/mm)
Load cycle number, N
0
1
2
3
4
5
6
0
20000
40000
60000
80000
100000

Figure 9

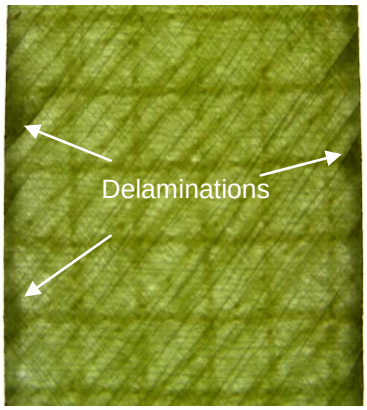

Figure 10

Table 1. Tensile properties of the epoxy polymers and GFRP composites.

Material	Condition	Tensile Properties		
		UTS (MPa)	Modulus, E (GPa)	Failure strain (%)
Epoxy polymers	Neat epoxy	73.3 ± 1.44	2.62 ± 0.05	3.78 ± 0.16
	Hybrid epoxy	64.4 ± 0.38	2.35 ± 0.06	4.61 ± 0.19
GFRP composites	Neat matrix	364.8 ± 13.1	17.50 ± 0.60	2.63 ± 0.11
	Hybrid matrix	380.3 ± 10.6	15.85 ± 0.95	2.72 ± 0.21

Table 2. Fatigue properties of the epoxy polymers and GFRP composites.

Material	Condition	Fatigue properties*	
		FSC (MPa)	FSE
Epoxy polymers	Neat epoxy	83.25	-0.1174
	Hybrid epoxy	98.71	-0.1095
GFRP composites	Neat matrix	462.48	-0.1121
	Hybrid matrix	534.81	-0.1079

* See the text for details of abbreviations